Available online at www.sciencedirect.com
SCIENCE DIRECT®
Journal of Hydrology 280 (2003) 246–264
Journal of Hydrology
www.elsevier.com/locate/jhydrol

Stream water infiltration, bank storage, and storage zone changes due to stream-stage fluctuations

Xi Chen[1], Xunhong Chen*

School of Natural Resource Sciences, University of Nebraska-Lincoln, 113 Nebraska Hall, Lincoln, NE 68588, USA

Received 9 January 2002; accepted 23 June 2003

Abstract

During a flood period, stream-stage increases induce infiltration of stream water into an aquifer; subsequent declines in stream stage cause a reverse motion of the infiltrated water. This paper presents the results of the water exchange rate between a stream and aquifer, the storage volume of the infiltrated stream water in the surrounding aquifer (bank storage), and the storage zone. The storage zone is the part of aquifer where groundwater is replaced by stream water during the flood. MODFLOW was used to simulate stream–aquifer interactions and to quantify rates of stream infiltration and return flow. MODPATH was used to trace the pathlines of the infiltrated stream water and to determine the size of the storage zone. Simulations were focused on the analyses of the effects of the stream-stage fluctuation, aquifer properties, the hydraulic conductivity of streambed sediments, regional hydraulic gradients, and recharge and evapotranspiration (ET) rates on stream–aquifer interactions. Generally, for a given stream–aquifer system, larger flow rates result from larger stream-stage fluctuations; larger storage volumes and storage zones are produced by larger and longer-lasting fluctuations. For a given stream-stage hydrograph, a lower-permeable streambed, an aquitard, or an anisotropic aquifer of low vertical hydraulic conductivity can significantly reduce the rate of infiltration and limit the size of the storage zone. The bank storage solely caused by the stage fluctuation differs slightly between gaining and losing streams. Short-term rainfall recharge and ET loss in the shallow groundwater slightly influence on the flow rate, but their effects on bank storage in a larger area for a longer period can be considerable.

Keywords: Flood stage; Bank storage; Storage zone; Stream–aquifer interactions

1. Introduction

Stream water infiltrates into a hydraulically connected aquifer during a rising flood stage and its reverse motion during streamflow recession recharges the stream; the volume of water so stored and released after the flood is referred to as bank storage (Fig. 1) (Singh, 1968; Todd, 1980). Bank storage may considerably attenuate the flood wave, decrease the peak discharge, and extend the hydrograph base time. Bank-storage effects can cause interpretive difficulties in connection with hydrograph separation. The magnitude of the infiltration rates and volumes of stored stream water are dependent on a number of

* Corresponding author. Tel.: +1-402-472-0772; fax: +1-402-472-4608.
[1] Present address: College of Water Resources, Hohai University, Nanjing, China
E-mail address: xchen2@unl.edu (Xunhong Chen).

0022-1694/03/$ - see front matter © 2003 Elsevier B.V. All rights reserved.
doi:10.1016/S0022-1694(03)00232-4

Nomenclature

Symbol definition [dimension (L, length; T, time)]

C_{riv}	Streambed conductance [L^2/T]
h_r	Flood-wave stage [L]
h_0	Maximum rise in stage [L]
h	Hydraulic head in the aquifer [L]
K_x, K_y, K_z,	Hydraulic conductivity of an unconfined aquifer in the x, y, and z directions, respectively [L/T]
K_{riv}	Hydraulic conductivity of streambed sediments [L/T]
M	Thickness of streambed [L]
Q_b	Flow rate between a stream and aquifer for a unit length of stream [L^2/T]
Q_{riv}	Flow rate between a stream and aquifer [L^3/T]
T	Duration of the flood wave [T]
t	Time [T]
t_c	Time of the flood crest [T]
t_p	Time when the infiltrated stream water begins to return to stream [T]
t_f	Maximum forward traveling period of infiltrated stream water [T]
V_{in}	Volume of infiltrated stream water into bank storage for a unit length of channel [L^2]
V_{out}	Volume of return flow from bank storage to the stream for a unit length of channel [L^2]
V_b	Volume of infiltrated stream water or return flow from bank storage to the stream for a unit length of channel [L^2]
W	Width of stream channel [L]

geologic and hydrologic parameters of the particular stream–aquifer systems.

Cooper and Rorabaugh (1963) provided an analytical solution to study the effect of asymmetric stage oscillation on infiltration rates and bank storage. Moench and Barlow (2000) presented Laplace transform step-response functions for various homogeneous confined and leaky aquifers and for anisotropic, homogeneous unconfined aquifers interacting with perennial streams. In their stream–aquifer model, the stream is assumed to penetrate the full thickness of the aquifer, and the infiltrated stream water during the flood is accumulated and stored on both sides of the stream. Barlow et al. (2000) applied the analytical step-response functions of Moench and Barlow (2000) to the analysis of stream–aquifer interactions along the Blackstone River in central Massachusetts and the Cedar River in eastern Iowa. Although these streams only partially penetrate the adjourning aquifers, the analysis for the Cedar River provided estimates of aquifer and stream-bank hydraulic properties and of recharge rates that were in close agreement with those estimated by more complex, multilayer numerical models. Zlotnik and Huang (1999) analyzed the sensitivity of the distribution of hydraulic heads to streambed properties

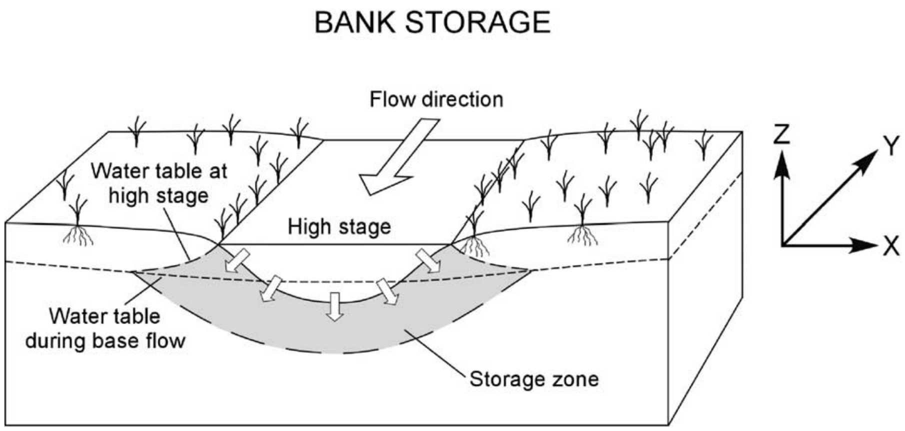

Fig. 1. Schematic diagram of bank storage Zone (modified from Winter et al. 1998).

based on an analytical solution for a stream–aquifer system where the stream channel partially penetrates and is imperfectly connected to the surrounding isotropic and homogeneous aquifers. Lal (2001) used Fourier analysis methods and complex variables to solve equations governing canal flow, groundwater flow, and the seepage between them. The analytical solution is valid in the isotropic aquifer and only when the sediment layer between the stream and the aquifer is relatively thin. A review of many other analytical solutions developed for the interaction of confined, leaky, and unconfined aquifers with an adjoining stream is provided by Barlow and Moench (1998). Pinder and Sauer (1971) studied the modification of a flood hydrograph due to bank storage effects based on numerical solutions of a coupled stream–aquifer system, which is described by partial differential equations of one-dimensional unsteady flow in full-penetration channels and two-dimensional groundwater flow. Examples of field investigation of groundwater discharge and bank storage during periods of overland runoff include Daniel et al. (1970).

These analyses, based on idealized flow systems, only partially reveal the interactions between the stream and aquifer during floods. Although infiltration rates and bank-storage volumes were analyzed, analyses were rarely done to determine the zone of aquifer where the infiltrated stream water had replaced the groundwater during the flood. While it is true that the infiltrated water accumulates horizontally within the stream banks, the water also accumulates in the aquifer beneath a shallow channel. Under this condition, the vertical hydraulic conductivity of stream sediments will play a role in the bank storage.

Singh (1968) noted that the flow of water from the stream into the banks depends on the relative positions of the stream stage and the groundwater tables, the boundary conditions, characteristic of the water-table profile, the hydraulic properties of the soil above the water table, the permeability of the soil–water interface at the bank, and the degree and intensity of stream-stage fluctuation. Because of the spatial variability in aquifer properties and the existence of partially penetrating stream channels, the infiltration flow in non-homogeneous and anisotropic aquifers is usually in three dimensions. The vertical flow is particularly strong in the part of the aquifer just beneath a stream. For a wide and shallow stream, such as the Platte River in Nebraska, USA, the area of the stream channel can be much greater than the lateral areas of both banks; thus, the exchange of stream water and groundwater occurs primarily in the vertical direction. Apparently, a significant portion of bank storage exists below the stream, and application of these analytical solutions to complex stream–aquifer systems could lead to a departure from the true results. In addition to the assumption of full penetration channels, most existing analytical solutions do not take into account the recharge, evapotranspiration (ET), or regional hydraulic gradients, although those of Moench and Barlow (2000) account for recharge or ET. Therefore, the effects of these hydrologic conditions on the bank storage deserve further analysis. Analysis of bank storage has a practical importance where a given level of streamflow is to be maintained for aquatic habitats by releasing water from upstream sources.

In addition, from the aspect of water-resource utilization and protection, water exchanged between the stream and the aquifer could cause inter-contamination between stream water and groundwater. Polluted stream water could infiltrate into the surrounding aquifers and contaminate the groundwater (Newsom and Wilson, 1988; Wilson, 1993). Therefore, the study of bank storage should be concerned not only with the rate and volume of stream infiltration in the aquifer but also on the area of aquifer that has been replaced by the stream water. In this study, we use the term storage zone to describe the maximum volume of aquifer through which infiltrated stream water migrates during the flood. In contrast to the traditional, somewhat limited concept of lateral bank storage (Cooper and Rorabaugh, 1963; Todd, 1980), in this work the storage zone includes the volume beneath the streambed, in addition to the area on the two sides of the channel.

In this study, we evaluated stream–aquifer interactions during a flood wave by use of numerical simulations. We designed a conceptual, three-dimensional stream–aquifer system for simulation of a series of scenarios that include varied flood-stage hydrographs, heterogeneous and anisotropic aquifers and related streambed hydraulic properties, regional hydraulic gradients, and rainfall recharge and ET from groundwater. Comparisons among the simulation results of these scenarios reveal the effects of the various conditions of the stream–aquifer system on bank storage, as well as the extension of the storage zone.

2. Methods

A rapid rise in stream stage that causes water to move from a stream into the streambanks and underlying sediments is usually caused by storm precipitation, rapid snowmelt, or release of water from an upstream reservoir. The loss of stream water to bank storage and return of this water to the stream tends to reduce flood peaks and later supplements stream flows (Winter et al., 1998). Methods for calculating the rate of water exchange, storage volume, and storage zone are described as follows.

2.1. Governing equations

Cooper and Rorabaugh (1963) suggested that the shapes of flood-wave stage hydrographs $h_r(t)$ might be approximated by one of the family of asymmetric curves defined by

$$h_r(t) = \begin{cases} Nh_0 e^{-\delta t}(1 - \cos \omega t), & \text{when } 0 \le t \le T \\ 0, & \text{when } t \ge T \end{cases} \quad (1)$$

where h_0 is the maximum rise in stage, t is the time since the beginning of the flood wave, T is the duration of the wave, $\omega = 2\pi/T$, $\delta = \omega \cot(\omega t_c/2)$ is a constant that determines the degree of asymmetry, t_c is the time of the flood crest, and

$$N = \frac{1}{e^{-\delta t_c}(1 - \cos \omega t_c)} \quad (2)$$

is a constant that serves to make the curves of the family peak at the same height h_0. Curves of $h_r(t)$ corresponding to $\delta = 0$, $\delta = 0.32\omega$ and $\delta = \omega$, or $t_c/T = 0.5$, $t_c/T = 0.4$ and $t_c/T = 0.25$ are shown in Fig. 2. The shapes of the stage hydrographs that accompany flood waves vary widely and depend upon the characteristics of the drainage basin, the areal and temporal distribution of the storm or snowmelt, and the rating curve of the stream at a given section

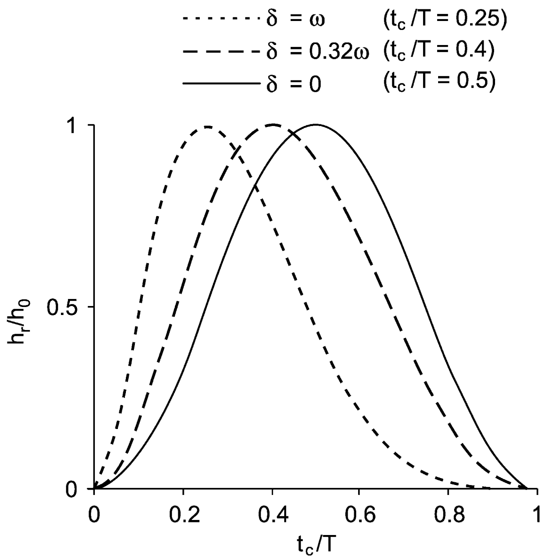

Fig. 2. Stream-stage hydrograph.

(Cooper and Rorabaugh, 1963) (see the nomenclature table for the dimensions of the symbols).

A higher or lower stream stage than adjacent groundwater levels during a flood period leads to infiltration of stream water into the surrounding aquifer or return of the infiltrated water to the stream. The rate of the flow between the stream and the aquifer is calculated from the difference in hydraulic heads in the stream and the adjacent aquifer using the following equation (McDonald and Harbaugh, 1988)

$$Q_{riv} = C_{riv}(h_r - h) \quad (3)$$

where Q_{riv} is the flow between the stream and the aquifer, h_r is the head in the stream described by Eq. (1), h is the head at the node in the cell underlying the stream reach, and C_{riv} is the hydraulic conductance of the stream–aquifer interconnection

$$C_{riv} = \frac{K_{riv} L_{riv} W}{M} \quad (4)$$

where K_{riv} is the hydraulic conductivity of the streambed sediments, L_{riv} is the length of the stream channel in the cell, W is the width of the stream channel in the cell, and M is the thickness of the riverbed material. A positive Q_{riv} indicates flow into the aquifer and negative Q_{riv} indicates flow into stream. We use Q_b to designate the flow rate for a unit length of stream channel.

The volume of stream water recharged into the aquifer for a unit length of channel (V_{in}) is calculated using

$$V_{in} = \int_0^{t_p} Q_b \mathrm{d}t \tag{5}$$

and the volume of return flow to the stream is (V_{out})

$$V_{out} = \int_{t_p}^{t} Q_b \,\mathrm{d}t \tag{6}$$

where t_p is the time when the bank storage reaches the maximum and the infiltrated stream water begins to return to stream, and t is an arbitrary time after the flood. Q_b is positive for $0 < t < t_p$, and negative for $t > t_p$. In the study, we use the term V_b to represent the cumulative volume of infiltrated stream water in the storage zone for a unit length of stream channel. V_b increases gradually for $0 < t < t_p$, reaches a maximum at $t = t_p$, and decreases for $t > t_p$ (see Fig. 3(b)).

If the stream is polluted, contaminated water particles penetrate into the aquifer during the rising flood stage. Thus, knowing the size and geometry of the storage zone is important to water quality management. By considering that the particles transported in groundwater only by advection and that diffusion is negligible, we can calculate the movement of particles using the average linear velocities of groundwater flow, V_x, V_y, and V_z, in the x, y, and z directions. The effective porosity of the aquifer is assumed to be equal to 0.2 in this study.

The US Geological Survey's MODFLOW (McDonald and Harbough, 1988; Harbaugh et al., 2000) was used to simulate the exchange of stream water and groundwater due to stream-stage fluctuations. MODFLOW is appropriate for simulation of groundwater flow in both confined and unconfined aquifers. The infiltration rates and volume of the recharged stream water to the aquifer are calculated during the flood, and the rate and volume of the return flow discharged from the stream to the aquifer are calculated for a period after the flood.

Determination of the storage zone is based on a particle-tracking package MODPATH (Pollock, 1989a,b, 1994). The pathlines and the final distribution of the infiltrated water particles are tracked to estimate the extent of the storage zone.

2.2. Design of stream–aquifer models

The dimension of the model domain is 5000 m in length (x direction), 5000 m in width (y direction), and 35 m in thickness (z direction). In the x direction, perpendicular to the stream channel, node spacing ranges from 5 m in the vicinity of the stream to 50 m near the boundary; finer finite-difference grids are used in the vicinity of the stream for more accurate tracking of the movement of the infiltrated stream water in the stream banks and the underlying sediments. In the z direction, the aquifer is divided into 10 layers. The top layer is 8 m thick and includes a 5 m vadose zone above the saturated portion. The thickness of the other nine layers is uniformly 3 m. The stream channel, which partially penetrates the aquifer and is parallel to the y direction, is assumed to be 50 m wide and 3 m deep in the beginning of the flood periods, and a streambed of 1 m thick is assumed. Grid spacing along y is arbitrarily 50 m because the groundwater flow is approximately perpendicular to the stream. The domain has 230 columns in the x direction and 100 rows in the y direction.

In the model, the variation of stream stage is determined using Eq. (1). The simulation period is equal to T plus an additional 25 days for simulating the bank storage returning into the stream. Time steps are 0.25 day during the flood period and gradually increase to a maximum length of 2.5 days during the non-flood period.

We placed water particles uniformly along the stream–aquifer interface: 26 particles in the streambed and five particles on each of the two lateral banks. The particles were released at the time when stream stage begins to rise. The pathlines are simulated by tracking particles from one cell to the next. Because the hydraulic gradient is nearly zero along the y direction, the water particles migrate dominantly in the vertical profile (the x–z cross-sections).

2.3. Scenarios of variation of flood stages and aquifer properties

A variety of stream–aquifer scenarios were simulated for the analysis of the characteristics of stream

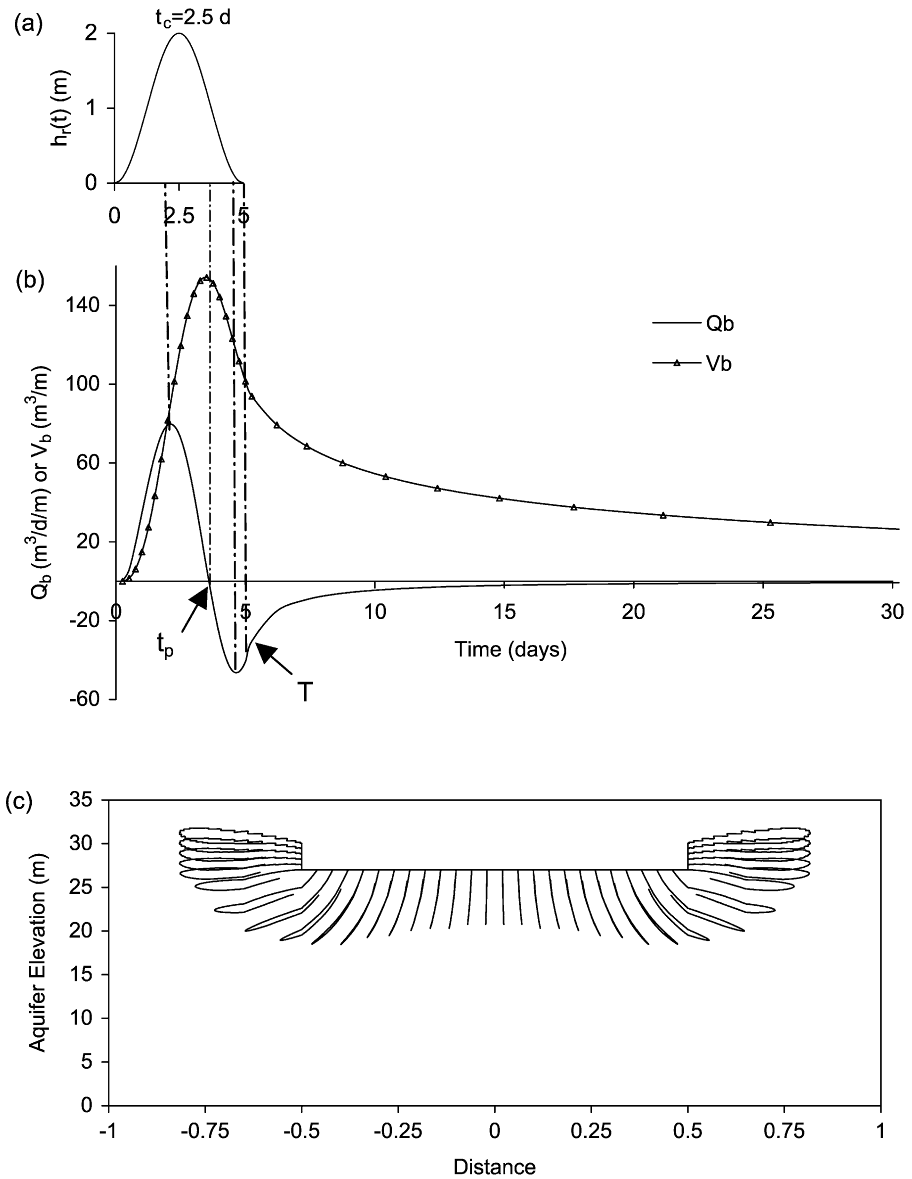

Fig. 3. Flood hydrograph (a), simulated flow rate (Q_b) and bank storage (V_b) (b), and pathlines of the infiltrated water particles over a vertical profile (c) with $h_0 = 2$ m, $t_c = 2.5$ d, and $t_c/T = 0.5$; $K_x = K_y = K_z = 100$ m/d. One unit length in the horizontal axis = 50 m.

water and groundwater exchanges. Three parameters, t_c, T, and h_0 in Eq. (1) control the stage variations. The time of the flood crest, t_c, ranges from hours to days and depends on the size and other characteristics of the basin, as well as the intensity of rainfall (Martinec, 1995). For small and medium-size drainage basins, t_c may vary from a few hours to 30 or 40 h (Singh, 1968); for large drainage basins, t_c may be as long as a few days. In this study, the following scenarios were made: t_c ranged from 0.5 to 3.5 days; shapes of the flood-stage hydrographs were either symmetrical ($t_c/T = 0.5$) or asymmetrical ($t_c/T < 0.5$); correspondingly, T rannged from 1 to 7 days; and the maximum rise in stage h_0 varied from 0.5 to 2 m.

Water exchanges between the stream and aquifers, and particle movements within the aquifer, are controlled by aquifer properties. Among the several aquifer parameters, hydraulic conductivity, K, plays a key role in controlling groundwater flow. The following scenarios were considered: homogeneous aquifer with K ranging from 1 to 100 m/d; non-homogenous aquifer with the second layer just below the streambed having a K from 0.1 to 10 m/d (aquitard), and the other nine layers with $K = 100$ m/d; anisotropic aquifer with K_x/K_z from 5 to 20; and a streambed sediment that impacts the hydraulic connection between the stream and the aquifer with the vertical hydraulic conductivities (K_{riv}) from 0.1 to 100 m/d. A strong anisotropy of alluvial aquifers in the Platte and Republican River valleys, Nebraska, USA, has been reported by Chen (1998), Ayers et al. (1998), McGuire and Kilpatrick (1998) and Chen et al. (1999). These simulations assume that the initial groundwater level is the same as the stream stage.

In addition, gaining and losing streams are also considered in our simulations. When the stream is gaining, rise of flood stage results in a reverse hydraulic gradient from the stream to the aquifer, and stream infiltration will not occur until the establishment of the reversal of the hydraulic gradient. The rise of flood stage will increase the existing infiltration rate in a losing stream. Because stream-stage variations often occur simultaneously with recharge or ET, we further analyzed the influences of areal recharges and ET on the bank storage.

3. Results

3.1. Simulation procedures and verification

Given a stream stage hydrograph and a stream–aquifer model, Q_{b}, V_{b}, and the size of the storage zone can be calculated using the outputs from MODFLOW and MODPATH. The example below illustrates the simulation results based on the following assumptions of the stream–aquifer system: the groundwater table and stream stage are flat before the flooding; the stream stage is initially the same as the horizontal groundwater levels and then varies according to the stream-stage hydrograph with $t_{\mathrm{c}} = 2.5$ d, $t_{\mathrm{c}}/T = 0.5$, and $h_0 = 2$ m (Fig. 3(a)); the unconfined aquifer is homogeneous and isotropic with $K = 100$ m/d; the stream partially penetrates the aquifer and is initially 3 m deep; the streambed has the same hydraulic conductivity as the aquifer; and the increase in saturated thickness of the aquifer due to flooding is small compared with the initial saturated thickness.

Q_{b} and V_{b} are shown in Fig. 3(b). The positive Q_{b} represents stream infiltration during the flood, and the negative Q_{b} indicates the return flow of the infiltrated water to the stream that begins in the later period of the flood and continues into the post-flood period. The return flow has lower rates, but lasts much longer than the period of stream infiltration. The largest rate of stream infiltration Q_{b} occurs earlier than the peak stage, and the largest rate of the return flow occurs in the stage recession period between t_{p} and T. Fig. 3(b) also reflects the variation of V_{b} due to stream stage oscillation. V_{b} reaches the maximum at $t = t_{\mathrm{p}}$, after which return flow begins. At time t_{c}, the hydraulic gradient is from the stream to the aquifer and the stream continues to recharge the aquifer. When the time reaches t_{p}, the hydraulic gradient is about to reverse and the infiltrated stream water to discharge back to the stream. t_{p} is often larger than t_{c}, which indicates that the infiltrated water continue to migrate forward under the influence of the hydraulic gradient from the stream to the aquifer during a short period of time when the stream stage begins to decline. Consequently, the accumulated stream water in the aquifer reaches the largest after the occurrence of peak stream stage.

The pathlines of the infiltrated stream water particles are shown in Fig. 3(c). The horizontal distance (in the x direction) is normalized according to the stream width; one normalized unit represents 50 m. During the flood period, when the flood stage rises higher than the adjacent groundwater levels, stream water infiltrates into the surrounding aquifer and moves away from the stream; after the flood stage declines, the infiltrated water moves back toward the stream. Fig. 3(c) indicates that the pathlines of the forward movement of infiltrated water do not fully overlap those of the water flowing back to the stream. The forward and backward movements of the infiltration water particles in the aquifer due to the flood form a storage zone, whose maximum extent is determined from the maximum traveling distance in a forward traveling period of each water particle. Connecting the location of each water particle at a given time gives a line (or front line) that indicates the size of the storage zone; the maximum storage zone is formed when the water particles begin to reverse their forward movement. The forward traveling period, t_f, also represents the time when the farthest infiltrated particles begin to return toward the stream. In contrast, t_p is the approximate time when the water particles nearest the stream boundary begin to return to the stream. Therefore, the difference between t_f and t_p is a measure of the time lag of flood wave propagation in the aquifer, which reflects effects of aquifer properties on bank storage.

Because Q_b, V_b, extent of the storage zone, and t_p fully describe the characteristics of water exchanges between the stream and the aquifer during the flood stage fluctuation, they are used to measure the interactions between the stream and aquifer due to a flood. For this base simulation, the maximum positive Q_b is 79.27 (m^2/d), and the maximum V_b is 154.21 (m^2). After 30 days, about 17% of infiltrated stream water remains in the aquifer (Table 1).

To evaluate the accuracy of the results from the numerical modeling, we chose the analytical solutions developed by Cooper and Rorabaugh (1963) to calculate the flow rates. We redesigned the stream–aquifer model where the stream channel fully penetrates the aquifer. The flow rates calculated from the analytical solutions by Cooper and Rorabaugh (1963) were compared with those from MODFLOW output. The curve obtained from the analytical solution satisfactorily matched the corresponding curve from the numerical solution by MODFLOW. When the Cooper and Rorabaugh solutions are used to approximate the flow rates between a partial penetrating stream and the aquifer, the results can be either underestimated for a wide stream or overestimated for a narrow stream and an anisotropic aquifer.

3.2. Effects of flood stage variation

We analyzed how the shapes of flood hydrograph, described by t_c, T, and h_0, affect bank storage in a homogeneous and isotropic aquifer with $K = 100 \times$ m/d. We used three flood-stage shapes, corresponding to $t_c = 1.25$, 2, and 5 days, with $T = 5$ days and $h_0 = 2$ m for each case.

The simulated results of Q_b and V_b shown in Fig. 4(b) and (c) indicate that, compared to the symmetrical hydrograph with $t_c = 2.5$ days (Fig. 4(a)), the asymmetrical hydrographs with the sharper rises of the flood stage ($t_c = 1.25$ and 2.0 days) lead to larger infiltration rates (Fig. 4(b)) and, correspondingly, a larger amount of stream water is accumulated in the surrounding aquifer for $t < 2.5$ d (Fig. 4(c)). Although the sharper rise of flood stage forms a larger peak rate of infiltration, the maximum amount of water storage in the aquifer is less because of a shorter rising time t_c.

The largest streamflow infiltration rates (positive peak discharge) occur at $t = 1$, 1.5, and 2 days for $t_c = 1.25$, 2, and 2.5 days, respectively (Fig. 4(b)). Therefore, these rates occur earlier than the highest flood stage for all three cases. This indicates that the largest hydraulic gradient from the stream to the aquifer occurs before the flood crest. The peak bank storage time t_p is 2.5, 3.25 and 3.75 days for $t_c = 1.25$, 2 and 2.5 days, respectively (Table 1).

Fig. 4(d) shows the maximum distances of the stream-water particles traveling in the aquifer for the three values of t_c, and indicates that the storage zone of stream water is proportional to t_c. The simulated results reveal that the time for particles to reach the maximum traveling distances (t_f) is the same as t_p in these scenarios, indicating that all infiltrated particles respond to the backward movements when the aquifer begins to discharge water into the stream.

For the flood duration $T = 1$, 3, 5, and 7 days, $t_c/T = 0.5$ and $h_0 = 2$ m, Fig. 5(a)–(c) shows that the shorter flood-waves (smaller T values) lead to larger rates of flow exchange between the stream and the aquifer, but a lower amount of water storage, apparently due to the intensity of flooding in a short period. Fig. 5(d) also demonstrates that, for the shorter stage-waves, stream infiltration influences a smaller area of the aquifer because the forward movements of the water particles occur in shorter periods.

For the flood period $T = 5$ days, simulations were conducted for $h_0 = 0.5$, 1, and 1.5 m, with $t_c = 2.5$ days. Results indicated that a larger h_0 gives larger Q_b

Table 1
Characteristics of Q_b, V_b and t_p for the Bank Storage (see the nomenclature table for the definition of symbols)

	Scenarios		Max ($+Q_b$)	Max ($-Q_b$)	Max (V_b)	V_b (30 d)/max (V_b)	t_p
Base simulation	[a]	$t_c = 2.5$ d	79.27	−45.97	154.21	0.17	3.75
Stream-stage hydrograph	t_c	1.25 d	111.23	−32.55	125.68	0.15	2.5
($K_x = K_y = K_z = 100$ m/d)	($h_0 = 2$ m, t_c /$T = 0.5$)	2.0 d	86.53	−38.4	147.64	0.17	3.25
	T	1 d	191.64	−117.04	73.56		0.75
	($h_0 = 2$ m,	3 d	102.18	−60.14	120.37		2.25
	$t_c/T = 0.5$)	7 d	64.74	−38.48	181.19		5
	h_0	0.5 m	19.52	−11.4	38.07	0.13	3.75
	($t_c = 2.5$ d,	1 m	39.25	−22.87	76.46	0.16	3.75
	$t_c/T = 0.5$)	1.5 m	59.16	−34.4	115.18	0.17	3.75
Aquifer hydraulic	K	1 m/d	13.96	−11.06	24.78	0.11	3.5
conductivities		10 m/d	28.72	−18.26	53.95	0.16	3.5
($h_0 = 2$ m, $t_c = 2.5$ d, $t_c/T = 0.5$)		100 m/d	79.27	−45.97	154.21	0.17	3.75
	K_x/K_z	5	69.43	−37.31	137.43	0.2	3.75
		10	62.16	−31.23	124.03	0.22	3.75
		20	53.34	−24.76	107.81	0.25	4
	K_2	0.1 m/d	7.86	−1.28	18.38	0.62	4.75
		1 m/d	34.14	−12.32	72.89	0.33	4.25
		10 m/d	66.64	−35.54	131.77	0.19	3.75
Streambed K	K_{riv}	0.1 m/d	8.91	−0.74	21.48	0.67	5
($h_0 = 2$ m, $t_c = 2.5$ d, $t_c/T = 0.5$,		1 m/d	35.39	−12.51	96.26	0.26	4.25
$K_x = K_y = K_z = 100$ m/d)		10 m/d	73.93	−41.51	145.8	0.18	3.75
Regional hydraulic gradients	I	0.001	69.37	−37.33	137.3	0.2	3.75
($h_0 = 2$ m, $t_c = 2.5$ d, $t_c/T = 0.5$,		0.003	69.23	−37.37	136.96	0.19	3.5
$K_x = K_y = 100$ m/d , $K_x/K_z = 5$)		−0.001	69.48	−37.30	137.56	0.21	3.75
		−0.003	69.6	−37.27	137.83	0.21	4
Recharge	R	$r = 10$ mm/d	68.76	−37.67	135.38	0.15	3.75
($h_0 = 2$ m, $t_c = 2.5$ d, $t_c/T = 0.5$,		$r = 20$ mm/d	68.1	−38.02	133.34	0.1	3.75
$K_x = K_y = 100$ m/d, $K_x/K_z = 5$)							
ET	E	$E = 32$ mm/d	69.76	−36.93	138.29	0.24	3.75
($h_0 = 2$ m, $t_c = 2.5$ d, $t_c/T = 0.5$,		$E = 64$ mm/d	70.09	−36.55	139.15	0.27	3.75
$K_x = K_y = 100$ m/d, $K_x/K_z = 5$)							

[a] The base simulation was based on $h_0 = 2$ m, $T = 5$ d, and $K_x = K_y = K_z = 100$ m/d.

and V_b values, but the values of t_p and the forward travel period, t_f, are the same for each of the three cases (Table 1).

3.3. Effects of hydraulic conductivities

According to Darcy's law, the rate of groundwater flow depends on the magnitude of hydraulic conductivity K, the relative differences among its principal components $K_x, s\,K_y$, and K_z, and the relative differences among $K_1, K_2, \ldots, K_{10}$ of the individual layers. Simulations were conducted to analyze how the hydraulic conductivities affect the rate, volume, and storage zone for a constant flood stage hydrograph with $T = 5$ days, $t_c/T = 0.5$ and $h_0 = 2$ m.

For three homogenous and isotropic aquifers with $K = 1$, 10 and 100 m/d, simulation results indicated that Q_b and V_b are proportional to hydraulic conductivities K. When K increases from 1 to 10 m/d, the positive peak values of Q_b and V_b are

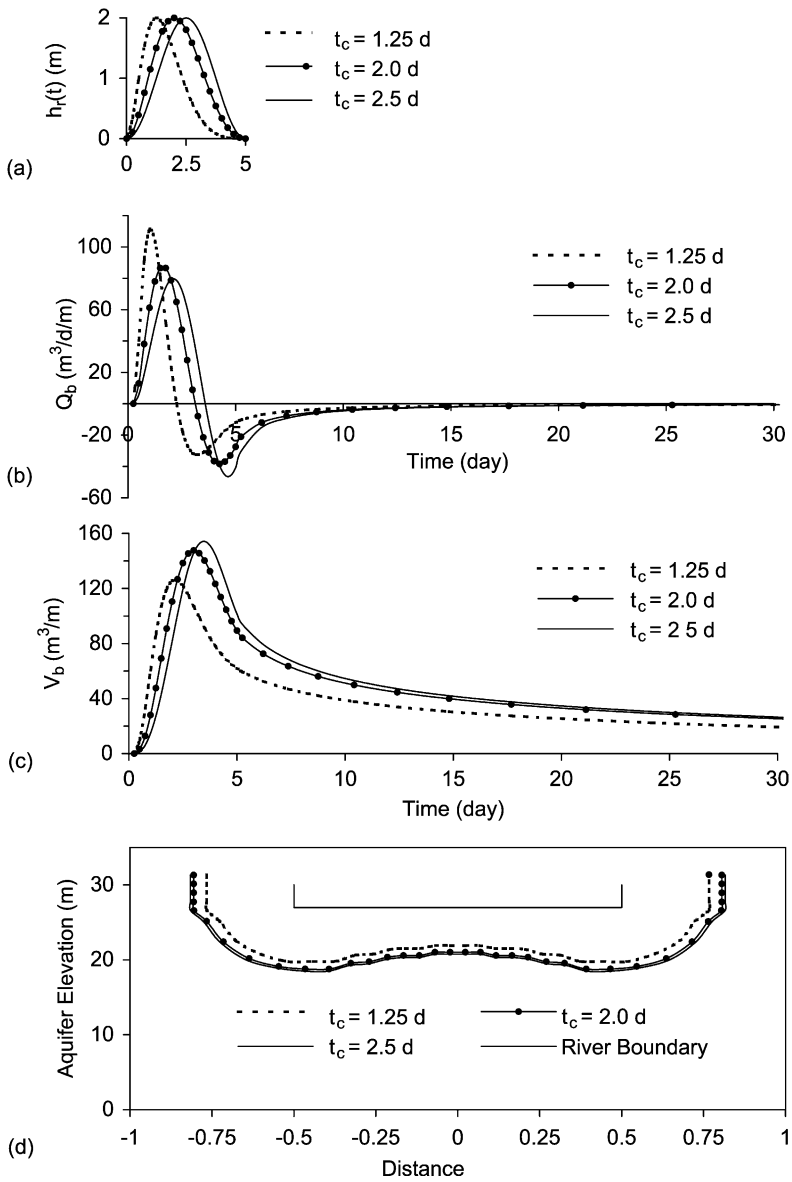

Fig. 4. Flood hydrograph (a), variation of flow rate (b), bank storage (c) and storage zone (d) due to variations in time of the flood crest (t_c). $h_0 = 2$ m, and $T = 5$ d; and $K_x = K_y = K_z = 100$ m/d.

approximately doubled, and negative peak of Q_b increases by 1.7 times; when K increases from 10 to 100 m/d, the positive peak values of Q_b and V_b increase by 2.8 times, and the negative peak of Q_b increases by 2.5 times. t_p is 3.5 days for $K = 1$ and 10 m/d, and 3.75 days for $K = 100$ m/d; note that t_c is 2.5 days. The storage zone expands more extensively both laterally and vertically with an increase in the value of K. The forward traveling period t_f is 1 and 0.25 day later than t_p for $K = 1$ and 10 m/d, respectively, and is equal to t_p for $K = 100$ m/d; this indicates that the propagation of the flood-wave in

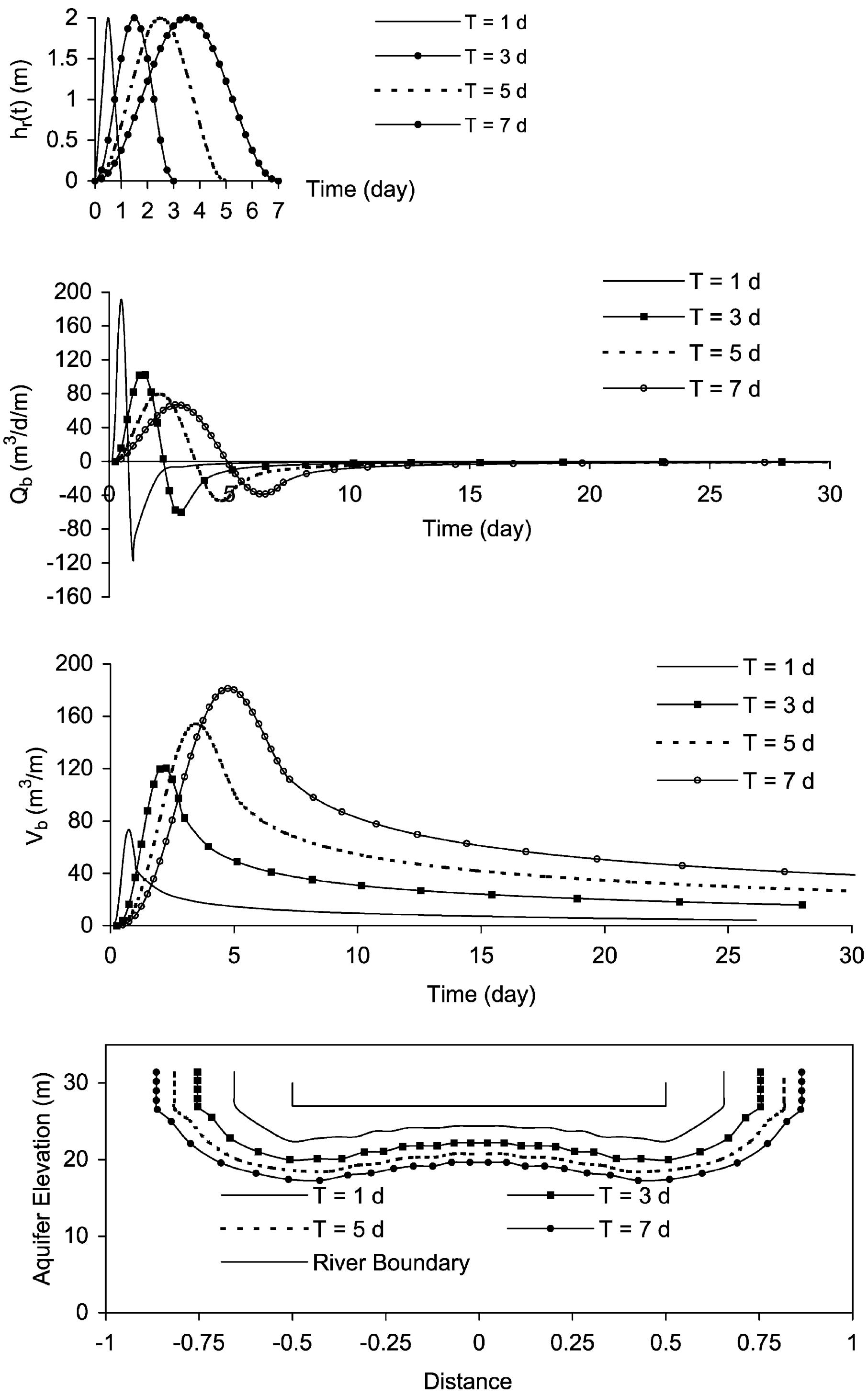

Fig. 5. Flood hydrograph (a), variation of flow rate (b), bank storage (c), and storage zone (d) due to variations in flood wave durations. $h_0 = 2$ m, $t_c/T = 0.5$, and $K_x = K_y = K_z = 100$ m/d.

the aquifers with lower values of hydraulic conductivity has a large time lag in response to the oscillation of flood stage.

For three homogenous and anisotropic aquifers with $K_x = K_y = 100$ m/d and $K_x/K_z = 5, 10$ and 20, Fig. 6(a) and (b) shows that Q_b and V_b are proportional to K_z, or inversely proportional to K_x/K_z. This is because the vertical flow component below the stream is strong and a smaller K_z value reduces the water exchange rates between stream and aquifer. Fig. 6(c) shows that when K_z is smaller than K_x, movement of the infiltrated water is restricted in the vertical direction, but its extension is magnified in the horizontal directions perpendicular to the stream. t_p is 4 days for $K_x/K_z = 20$, and 3.75 days for $K_x/K_z = 1, 5$, and 10. As shown in Fig. 6(b), V_b at $t = 30$ days is nearly identical for each of the four cases, although the maximum V_b differs greatly among them. Thus, a stronger anisotropy reduces the amount of infiltrated water. The ratio of V_b at $t = 30$ days to the maximum V_b (see Table 1) indicates that about 1/4 of bank storage remains in the storage zone for $K_x/K_z = 100$, compared to less than 1/5 for $K_x/K_z = 1$.

Additional simulations were conducted for the non-homogenous but isotropic aquifers in which the hydraulic conductivity K_2 in the second layer, just below the streambed, is assumed to be 0.1, 1, and 10 m/d, smaller than those in the other nine layers $K_1 = K_3 = \ldots = K_{10} = 100$ m/d. Fig. 7(a) and (b) indicates that the lower permeable layer, just beneath the river channel, significantly impedes water exchanges between the stream and aquifer. For example, when $K_2 = 10$ m/d, the maximum $V_b = 131.77$ (m^3/m), compared to $V_b = 18.38$ (m^3/m) when $K_2 = 0.1$ m/d (Table 1). Moreover, the lower permeable layer postpones propagation of the flood-waves in the aquifer and results in the positive peak of Q_b occurring at later times (2, 2.25, 2.5, and 2.75 days for $K_2 = 100$, 10, 1 and 0.1 m/d, respectively), and t_p being correspondingly larger (3.75, 3.75, 4.25 and 4.75 days for $K_2 = 100$, 10, 1 and 0.1 m/d, respectively). The return of infiltrated water due to a low K_2 is also very slow. Fig. 7 (c) indicates that water movements in the vertical direction are restricted by a low-permeability layer. For example, when K_2 is equal to 0.1 m/d, water particles could move in the horizontal direction from both sides of the stream channel but did not infiltrate through the low-permeability layer; and the forward traveling period, t_f, is 5.25 days for the particles in the stream banks but as large as 12.4 days for particles that have migrated downward, which indicates that the lower-permeability layer results in insensitive response of the infiltrated water to the flood stage variation. When $K_2 = 0.1$ m/d, the ratio of V_b ($t = 30$ days) to V_b (maximum) indicates that 62% of infiltrated stream water remains in the storage zone (Table 1); this value reduces to 32% for $K_2 = 1$ m/d, and 19% for $K_2 = 10$ m/d.

The hydraulic conductivity of streambed sediments is another parameter affecting the hydraulic connection between the stream and aquifers. Four simulations with the K_{riv} values of 0.1, 1,10, and 100 m/d were conducted. The analysis of the streambed differs from the analyses of a low-permeability aquifer layer discussed above because the streambed is limited only in the channel. The simulated results of Q_b and V_b shown in Fig. 8(a) and (b) indicate that the less permeable sediments in the streambed have a similar role as a low-permeability aquifer in reducing streamflow into the aquifer. But the effect of the smaller K_{riv} to Q_b and V_b is not as significant as that of smaller K_2 if K_{riv} and K_2 both have the same value. t_p is 5, 4.25, 3.75 and 3.75 days for $K_{riv} = 0.1, 1, 10$ and 100 m/d, respectively, which means that the lower permeability sediments delay the inception of return flow. Fig. 8(c) shows that the storage zone expands in both the horizontal and vertical directions with the increase of K_{riv}. A low-permeability streambed also significantly reduces the rate of the return flow (Table 1); the infiltrated stream water remains much longer in the storage zone.

3.4. Effects of regional hydraulic gradients and climatic conditions

For a gaining stream, groundwater discharge decreases with the beginning of a stream rise, ceases after a short interval, and then bank storage occurs (Daniel et al., 1970). To analyze influences of the regional hydraulic gradient on bank storage due to flood-stage oscillation, we generated steady-state groundwater flow based on the following conditions of a hypothetical stream–aquifer system: the aquifer is homogeneous and anisotropic with

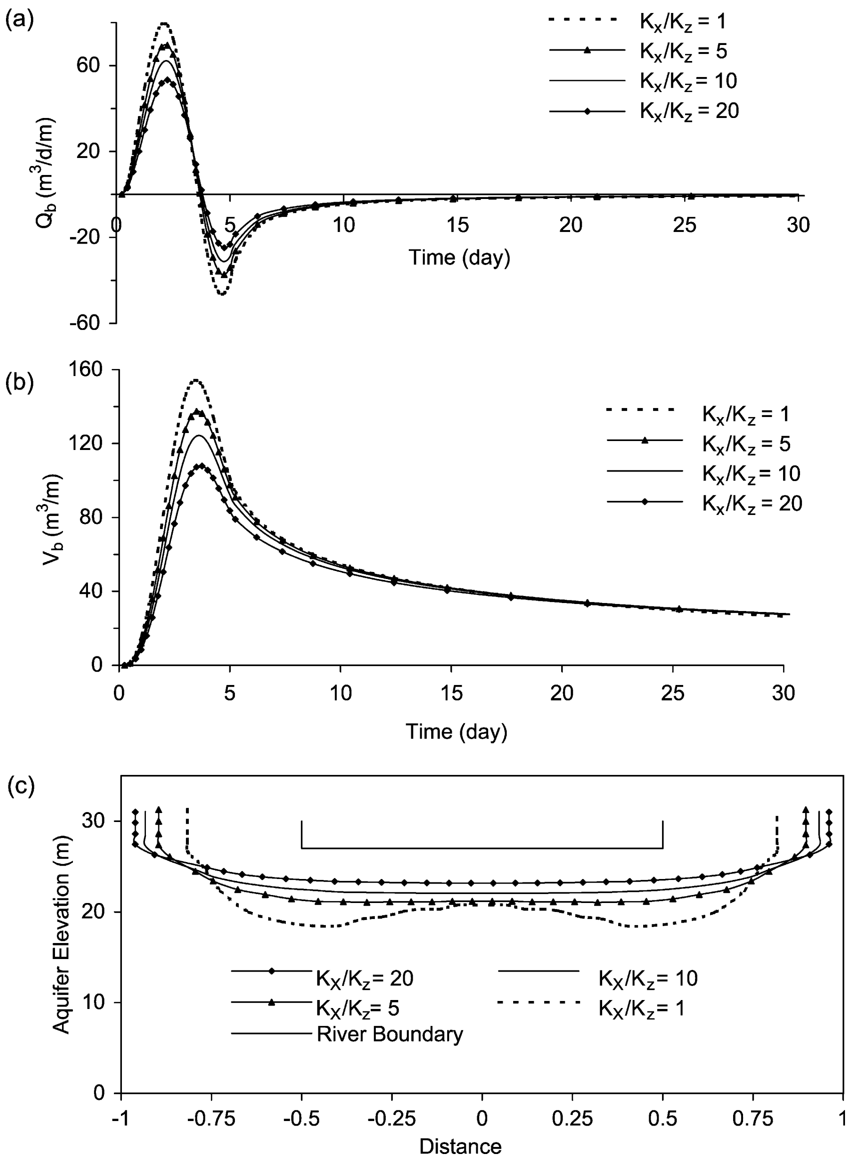

Fig. 6. Variation of flow rate (a), bank storage (b) and storage zone (c) due to variations in the anisotropy of the aquifer (K_x/K_z). $h_0 = 2$ m, $t_c = 2.5$ d and $t_c/T = 0.5$; and $K_x = K_y = 100$ m/d.

$K_x = K_y = 100$ m/d and $K_x/K_z = 5$; initial groundwater levels are uniform at a 30-m height; and groundwater levels in the two domain boundaries, parallel to the stream, are 35-m high, higher than the stream stage of 30 m. After running MODFLOW for a simulation period of 800 days with a constant stream stage, the obtained groundwater head distribution is considered to be near a steady-state condition. The slope of the generated groundwater surface (or the hydraulic gradient I) in the vicinity of the stream is about 0.003. With the same method, another groundwater surface with a gentler hydraulic gradient, $I = 0.001$, is generated when the boundary groundwater levels in the stream–aquifer system are

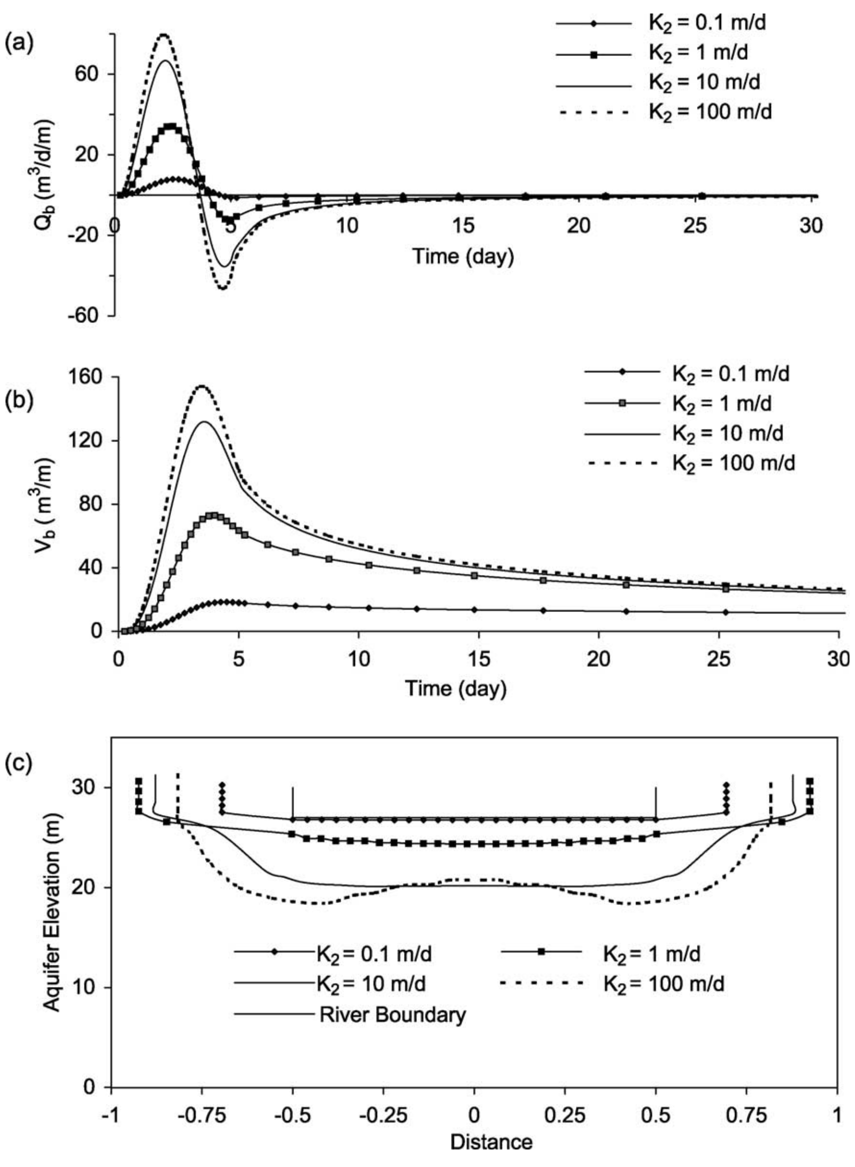

Fig. 7. Variation of flow rate (a), bank storage (b) and storage zone (c) due to variations in the hydraulic conductivity of layer 2 below the streambed (K_2). $h_0 = 2$ m, $t_c = 2.5$ d and $t_c/T = 0.5$; and $K_1 = K_3 = \ldots = K_{10} = 100$ m/d.

set at 31.5 m. Both I values can be considered as the regional hydraulic gradients that contribute groundwater to the stream as baseflow. Similar procedures were used to generate two hydraulic gradients, $I = -0.001$ and -0.003, near a losing stream. The generated groundwater heads are used as initial groundwater conditions for the next simulation in a flood period. The flood stage is characterized by $h_0 = 2$ m, $t_c = 2.5$ days and $t_c/T = 0.5$.

Obviously, under the combined effects of stream-stage variation and the regional hydraulic gradients, the infiltration rates from the gaining streams become smaller but the rates of return flow become larger. As a result, less bank storage is generated. The opposite is true for losing streams. Fig. 9(a) shows that the regional hydraulic gradients toward the stream restrict expansion of the storage zone. t_f is 3.75 days for $I = 0$; and t_f is 3.5 days when

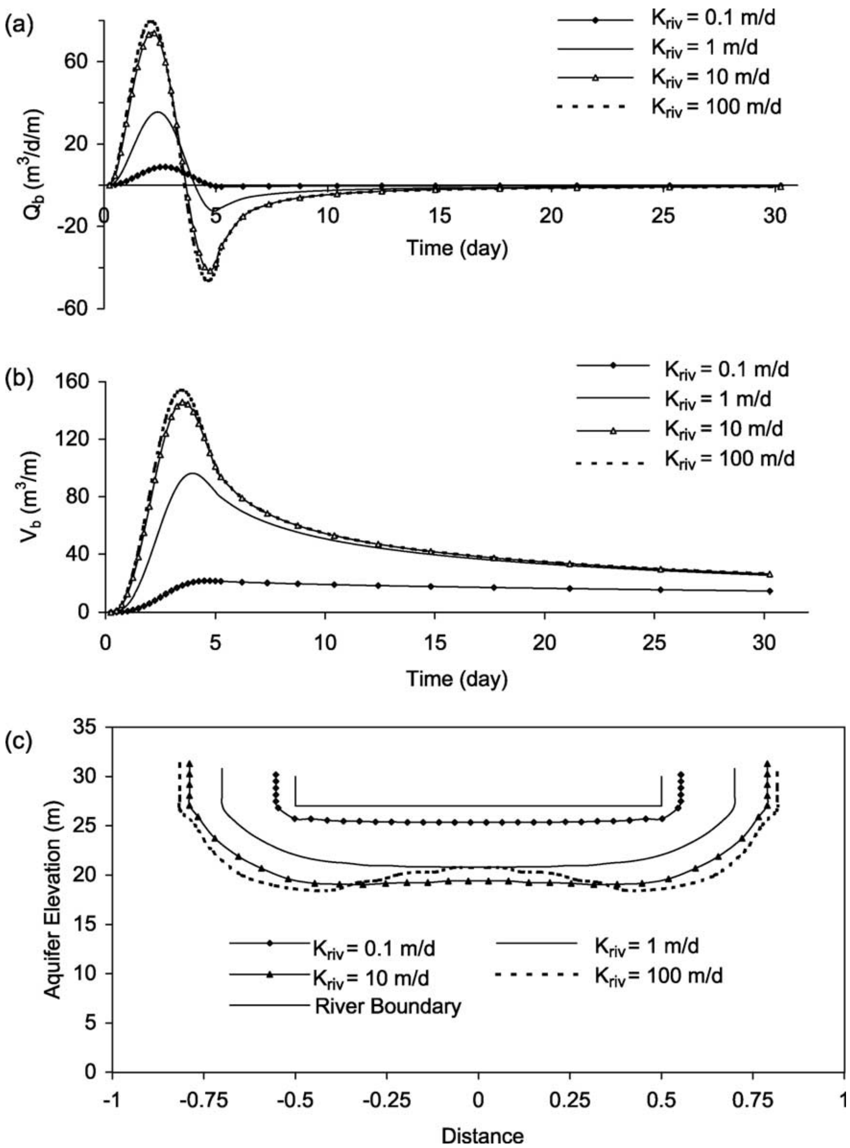

Fig. 8. Variation of flow rate (a), bank storage (b), and storage zone (c) due to variations in the hydraulic conductivity of streambed sediment (K_{riv}). $h_0 = 2$ m, $t_c = 2.5$ d and $t_c/T = 0.5$; and $K_x = K_y = K_z = 100$ m/d.

$I = 0.001$ and 2.5 days for $I = 0.003$. Both the t_f values for the gaining streams are smaller than their corresponding t_p values, and this suggests that the particles in the aquifer begin backward movements prior to the return flow. On the other hand, some of the earlier infiltrated stream water from the losing stream continues its 'one-way' movement for an entire 30-day period. Note that the water particles along the front lines (Fig. 9(a)) for the losing streams are those infiltrated at the earliest; some of the stream water infiltrated during the later period return to the stream after the time t_p.

Because a steady-state condition is assumed for the regional flow, a constant discharge from the aquifer to the gaining stream or a constant recharge from the stream to the aquifer is expected for a unit length of

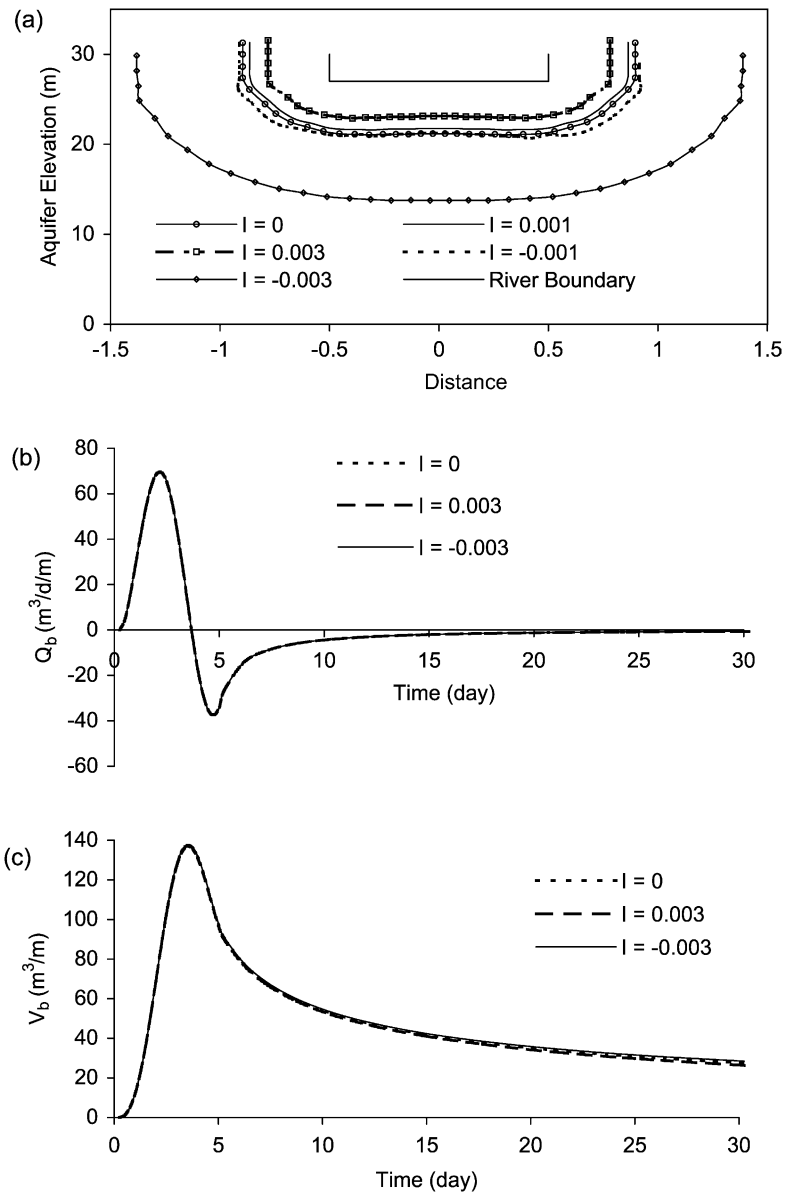

Fig. 9. Variation of flow rate (a), bank storage (b) and storage zone (c) due to variations in the regional hydraulic gradients near gaining (positive I) and losing (negative I) streams. $h_0 = 2$ m, $t_c = 2.5$ d and $t_c/T = 0.5$; $K_x = K_y = 100$ m/d and $K_x/K_z = 5$.

stream. If we discount the regional flow in the flow rates, we are able to plot the curves of bank storage solely due to the flood (Fig. 9(b) and (c), Table 1). Results in this figure show that either gaining or losing streams only slightly affects the rates of water exchanges and the bank storage that are solely caused by flood fluctuation.

We also simulated the effects of areal recharge and ET on the stream–aquifer interactions. The areal recharge is based on ideal conditions with a uniform recharge rate. If the flood stage rise was caused by precipitation, the recharge was concentrated in the relatively short time of the flood-rising period.

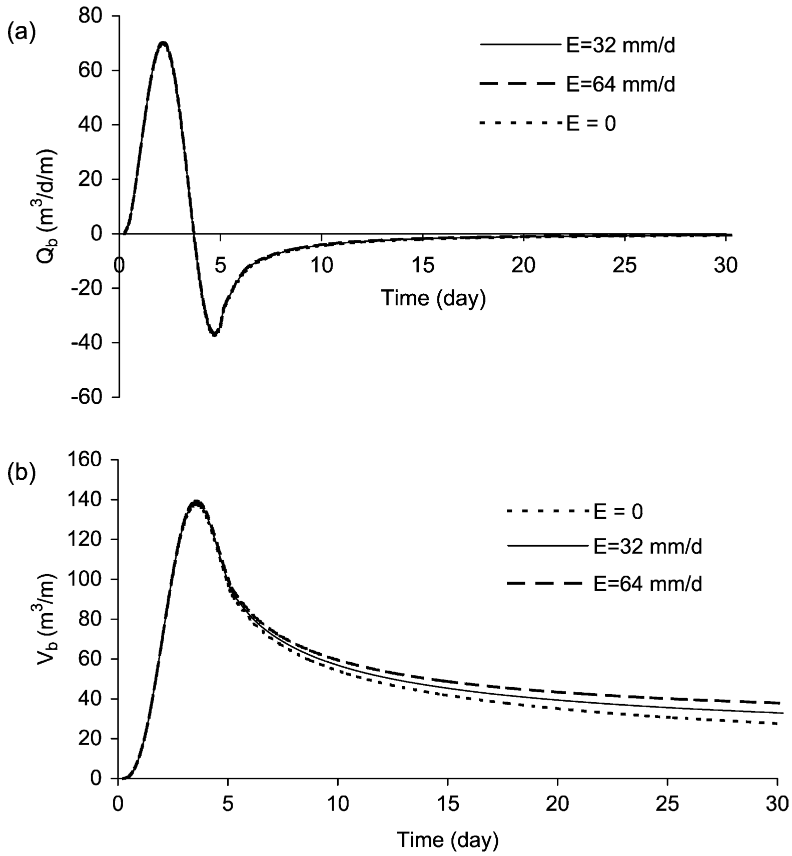

Fig. 10. Variation of flow rate (a) and bank storage (b) due to ET (E). $h_0 = 2$ m, $t_c = 2.5$ d and $t_c/T = 0.5$; $K_x = K_y = 100$ m/d and $K_x/K_z = 5$.

Two recharge rates, $r = 10$ and 20 mm/d, were considered in separate simulations over the model domain, and each recharge lasts 2 days in the beginning of the flood period. Because the recharge takes a relatively short time, its effect on the stream infiltration and return flow is not significant; however, a notable effect can be observed on the cumulative volume (bank storage), particularly in the time when return flow has occurred. After 30 days, 15 and 10% of infiltration water remains in the aquifer for $r = 10$ mm/d and 20 m/d, respectively (Table 1).

ET was applied to the model and was simulated using the ET package of MODFLOW based on the ground surface elevation SURF = 35 m, maximum potential ET rates $E = 32$ and 64 mm/d, and the extinction depth EXDP = 5 m. Because the initial depth from the ground surface to water table is 5 m, ET plays a role only when the water level rises due to flooding in the stream. The simulated results are shown in Fig. 10(a) and (b). Again, the effect on the flow rate Q_b is not important (Fig. 10(a)), but the cumulative effect on the bank storage V_b can be noticed in the period of return flow (Fig. 10(b)). Note that this bank storage represents infiltrated water, and part of it has evaporated due to the rise of the groundwater table in the flood period. As shown by Fig. 10(b) and listed Table 1, for a higher potential ET rate, slightly more stream water infiltrated into the aquifer, but more bank storage was lost to ET, e.g. the water loss through ET per unit length of stream channel in 30 days is 10.5 m^3 and 19.6 m^3 for $E = 32$ and 64 mm/d, respectively, which are about 7 and 14% of the total infiltrated water during the flood, respectively. For a stream reach that is many miles long, the volume of the lost bank storage due to ET may be very significant.

4. Summary and conclusions

Traditionally, flow rate and bank storage have been two criteria used to measure the level of stream–aquifer interactions due to flood stages in stream. We added another criterion, storage zone, in this paper to reflect the hydraulic connectivity between stream and aquifer. Our simulation results suggest that the characteristics of flood hydrograph, the geometry of stream channel, and the aquifer hydraulic properties can play an important role in affecting the rate and volume of stream infiltration and return flow, as well as the size and shape of a storage zone. The storage zone is not located solely on both sides of a stream; a significant portion of the zone can exist under the streambed of a partially penetrating channel. The storage zone gradually reduces its size when the bank storage returns water to the stream. The infiltration process often exists in a much shorter period compared to the period of the return flow.

In a given aquifer system, a larger flow rate responds to a sharper rise or decline of the stream-stage. For a flood rising to higher stages and lasting longer periods, more stream water could infiltrate into the aquifer and form a larger storage zone in the aquifer. The largest infiltration rate occurs prior to the maximum rise in flood stage, and the maximum bank storage occurs before the end of the flood when infiltrated water begins to return into the stream (return flow). If there are no regional hydraulic gradients, the maximum extension of the storage zone is formed just at or after the beginning of the return flow.

For a given hydrograph, a larger flow rate, as well as storage volume and storage zone, are formed in highly permeable aquifers that better connect with the stream, and smaller flow rates and storage volumes indicate otherwise. Each of these systems, an aquitard layer interbedded with highly permeable aquifers, a strong anisotropic aquifer of small vertical hydraulic conductivity, and lower permeability aquifers, can reduce the flow rate and bank storage. The lower hydraulic conductivity of a streambed or lower permeability aquifer restricts the extension of the storage zone in the area both below the channel and in the river banks. An aquitard and a strong anisotropic aquifer reduce the extension of the storage zone in the area below the channel but can increase its extension laterally in the river banks.

The regional hydraulic gradients themselves significantly influence stream water infiltration and storage zone in the aquifer but seem to have little effect on flow rate and bank storage that are solely caused by flood in streams. While areal recharge can increase return flow to the stream; the effect of ET goes oppositely. Although the changes of flow rates that have been caused by ET are not significant for a unit length of channel, the total effect for a long reach of the stream in a long dry period might significantly reduce infiltrated water. Thus, attention should be paid to the loss of bank storage due to ET in the practice of maintaining inflow in rivers.

Acknowledgements

The research was supported by the US Geological Survey and the Water Center and Conservation & Survey Division at University of Nebraska-Lincoln. C. Flowerday provided editorial review. Two anonymous reviewers provided useful comments for improving the quality of the paper. The content of the paper does not necessarily reflect the views of the USGS. The findings presented herein are those of the authors.

References

Ayers, J.F., Chen, X.H., Gosselin, D., 1998. Behavior of nitrate–nitrogen movement around a pumping high-capacity well: a field example. Ground Water 36 (2), 325–337.

Barlow, P.M., Moench, A.F., 1998. Analytical solutions and computer programs for hydraulic interaction of stream–aquifer systems, US Geological Survey Open-File Report 98-415A, pp. 85.

Barlow, P.M., DeSimone, L.A., Moench, A.F., 2000. Aquifer response to stream-stage and recharge variations II. Convolution method and applications. Journal of Hydrology 230, 211–229.

Chen, X.H., 1998. Assessment of hydraulic properties from an alluvial aquifer near Grand Island, Nebraska. Journal of American Water Resources Association 24 (3), 603–616.

Chen, X.H., Goeke, J., Summerside, S., 1999. Hydraulic properties and uncertainty analysis for an unconfined alluvial aquifer. Ground Water 37 (6), 845–854.

Cooper, H.H., Rorabaugh, M., 1963. Groundwater movements and bank storage due to flood stages in surface stream. US Geol. Survey Water Supply Paper 1536-J, 343–366.

Daniel, J.F., Cable, L.W., Wolf, R.J., 1970. Ground water-surface water relation during periods of overland flow. US Geological Survey Professional Paper 700-b, 219–223.

Harbaugh, A.W., Bantaa, E.R., Hill, M.C., McDonald, M.G., 2000. MODFLOW-2000, The US Geological Survey modular ground-water model—User guide to modularization concepts and the ground-water flow process, US Geological Survey Open-File Report, 00-92.

Lal, A.M.W., 2001. Modification of canal flow due to stream–aquifer interaction. Journal of Hydraulic Engineering 127 (7), 567–576.

Martinec, J., 1985. Time in Hydrology. In: Rodd, J.C., (ed.), Facets of hydrology, vol. II. Wiley, New York, 249–290.

McDonald, M.G., Harbaugh, A.W., 1988. A modular three-dimensional finite-difference ground-water flow model. US Geological Survey Techniques of Water-Resources Investigations, Book 6, Chapter A1, 586 p.

McGuire, V.L., Kilpatrick, J.M., 1998. Hydrogeology in the vicinity of the Nebraska Management Systems Evaluation Area (MSEA) site, central Nebraska, US Geological Survey Water-Resources Investigations Report 97-4266, 25 p.

Moench, A.F., Barlow, P.M., 2000. Aquifer response to stream-stage and recharge variations: I. Analytical step-response functions. Journal of Hydrology 230, 192–210.

Newsom, J.M., Wilson, J.L., 1988. Flow of groundwater to a well near a stream—effect of ambient groundwater flow direction. Ground Water 26 (6), 703–711.

Pinder, G.F., Sauer, S.P., 1971. Numerical simulation of flood wave modification due to bank storage effects. Water Resources Research 7 (1), 63–70.

Pollock, D.W., 1989a. Documentation of computer programs to compute and display pathlines using results from the US Geological Survey modular three-dimensional finite-difference ground-water flow model, US Geological Survey Open-File Report 89-381.

Pollock, D.W., 1989b. Documentation of GKS-based MODPATH-PLOT, US Geological Survey Open-File Report 89-622.

Pollock, D.W., 1994. User's Guide for MODPATH/MODPATH-PLOT, Version 3: A particle tracking post-processing for MODFLOW, the US Geological Survey finite-difference ground-water flow model, US Geological Survey Open-File Report 94-464.

Singh, K.P., 1968. Some factors affecting baseflow. Water Resources Research 4 (5), 985–999.

Todd D.K., 1980. Groundwater Hydrogeology, Wiley, New York, 535 p..

Wilson, J.L., 1993. Induced infiltration in aquifers with ambient flow. Water Resources Research 29 (10), 3503–3512.

Winter, T.C., Harvey, J.W., Franke, O.L., Alley, W.M., 1998. Ground water and surface water a single resource.U.S. Geological Survey Circular, 1139.

Zlotnik, V.A., Huang, H., 1999. Effect of shallow penetration and streambed sediments on aquifer response to stream stage fluctuations (analytical model). Ground Water 37 (4), 599–605.